Journal of Catalysis 329 (2015) 248–261

Contents lists available at ScienceDirect

Journal of Catalysis

journal homepage: www.elsevier.com/locate/jcat

Preferential oxidation of carbon monoxide over Pt–FeO_x/CeO_2 synthesized by two-nozzle flame spray pyrolysis

Jochen A.H. Dreyer [a], Henrike K. Grossmann [b], Jinfan Chen [a], Tim Grieb [b], Bill B. Gong [c], Patrick H.-L. Sit [a], Lutz Mädler [b], Wey Yang Teoh [a,*]

[a] *Clean Energy and Nanotechnology (CLEAN) Laboratory, School of Energy and Environment, City University of Hong Kong, Kowloon, Hong Kong Special Administrative Region*
[b] *Foundation Institute of Materials Science (IWT), Department of Production Engineering, University of Bremen, Germany*
[c] *Mark Wainwright Analytical Centre, Solid State and Elemental Analysis Unit, University of New South Wales, Sydney, Australia*

ARTICLE INFO

Article history:
Received 12 February 2015
Revised 29 April 2015
Accepted 6 May 2015
Available online 15 June 2015

Keywords:
CO oxidation
Preferential oxidation (PROX)
Flame spray pyrolysis
Temperature-programmed studies
Density functional theory

ABSTRACT

Pt–FeO_x–CeO_2 catalysts for the preferential oxidation of CO (CO-PROX) with controllable segregation between the Pt/FeO_x and CeO_2 components were synthesized by two-nozzle flame spray pyrolysis. This was achieved by flame-spraying the two active components independently in two interfacing flames. By adjusting the intersection distance between the two aerosol flames, it was possible to tune the morphology and the reducibility of the catalysts. Intimate interactions between Pt/FeO_x and CeO_2 (without oversintering the two components) achieved at the greatest flame distance gave reducibility at the lowest temperature, as corresponding to the formation of oxygen vacancies around the Pt (from H-spillover). Maximum CO conversion (>99.5%) for the two-nozzle synthesized catalysts was achieved below 90 °C, which is 30 °C lower than for mechanically mixed Pt/FeO_x and CeO_2. While high CO_2 selectivity was attained at lower temperatures, it was limited by the adsorption of reactive oxygen. The oxygen vacancies on the Pt–FeO_x–CeO_2 catalyst were gradually oxidized at low temperatures due to unconsumed O_2, and this led to a decrease in CO conversion with time on stream. In contrast, complete consumption of O_2 and excess of dissociated H_2 sustained the high oxygen vacancies content at high temperatures and hence high activity (although nonselective) was achieved. We further identified the loss of CO_2 selectivity at high temperature as originating from the weakened CO adsorption compared to that of H_2 in the presence of oxygen vacancies.

1. Introduction

Proton exchange membrane fuel cells (PEMFCs) are promising alternatives to combustion engines given their high efficiencies [1,2], low operating temperatures [3], and limited pollutant emission [4]. However, existing challenges such as the lack of infrastructure for hydrogen (H_2) distribution and storage [2,3] suggest the need for onboard H_2 generation by steam and/or autothermal reforming of hydrocarbons [1,3]. A drawback of the reforming process is that up to 10% carbon monoxide (CO) is formed alongside the desirable H_2 [5]. The CO would chemisorb on the Pt anode of the PEMFC, resulting in the deterioration of H_2-to-electricity conversion [6,7]. Onboard CO removal becomes necessary but the water–gas-shift (WGS) reaction can only reduce the CO concentration to 1000–10,000 ppm [5,8], instead of the required 10–100 ppm for the suitable PEMFC operation [8]. A leading solution for reducing the CO concentration in H_2-rich reformate gas to an amount tolerable by PEMFCs is the catalytic preferential oxidation (PROX). Here, the CO is selectively oxidized to CO_2, which is benign to PEMFCs. However, the key requirements for efficient CO-PROX catalysts are high CO conversion at temperatures between the WGS reaction and that of PEMFC operation, as well as high selectivity toward CO_2 with minimal H_2 oxidation [3,8–10].

To date, a variety of supported catalytic materials for CO-PROX have been reported, including Au/TiO_2 [10–12], Pt/Al_2O_3 [13–16], Pt/FeO_x [17–20], Pt–CeO_2 [9], and CuO/CeO_2 [21–24]. These PROX catalysts have unique mechanisms depending not only on the active metal sites, but also on their interaction or noninteraction with the support. For example, the oxidation of CO over supported Pt on irreducible Al_2O_3 is dictated by a relatively straightforward Langmuir-type adsorption onto the Pt surface [13–16]. The reaction mechanism becomes more complex for Pt dispersed on reducible supports such as CeO_2 and Fe_2O_3 [18–20]. Low-temperature

---

* Corresponding author. Fax: +852 2319 5927.
E-mail address: wyteoh@cityu.edu.hk (W.Y. Teoh).

http://dx.doi.org/10.1016/j.jcat.2015.05.003
0021-9517/© 2015 Elsevier Inc. All rights reserved.

reactions are often observed and related to the reducibility as well as the oxidation state of the supports. An often-proposed explanation is the ease of surface lattice oxygen transport to the metal–support interface, which provides an alternative low-energy route compared to direct dissociative adsorption of O_2 on Pt [14,17,20,25–29]. At the same time, the electronic interactions between Pt and the reduced support may alter the characteristics of the reactant adsorption [29–33]. For these reasons, the design of low-temperature PROX catalysts is often directed toward improving the reducibility of the support, for example, through the cationic dopant modification of CeO_2 to give FeO_x–CeO_2 solid solutions [27,28]. Not only did the lower valence of the dopant ions lead to the formation of oxygen vacancies due to charge compensation, but also the smaller ionic radii of the dopants weakened the metal–oxygen bonds and thus enhanced the support reducibility [34]. Manipulation of such physicochemical characteristics, when coupled with the knowledge of specific reaction mechanisms, is a powerful tool that leads to the discovery of new PROX catalysts.

Based on these design principles, we explore the synthesis of a novel Pt-based CO-PROX catalyst using the flame spray pyrolysis (FSP) [35,36]. FSP is a versatile technique for the synthesis of simple and composite metal oxides with assured stoichiometry, high specific surface area and good crystallinity [35–37]. In the past, we have used single-nozzle FSP to synthesize ready-to-use CuO/CeO_2 PROX catalysts with controllable 1–12 wt.% Cu loading [22–38]. Here, we report for the first time the synthesis of Pt–FeO_x–CeO_2 PROX catalysts using the two-nozzle FSP [39–43]. In contrast to conventional single-nozzle FSP, the Pt/FeO_x and CeO_2 components are sprayed simultaneously but through independent flames during the two-nozzle synthesis. This gives a high level of controllability over the resultant morphology, be it heavily doped composite oxide or separate oxide phases, which in turn gives direct control over the reducibility of the catalysts. We further clarified the PROX activity and selectivity in relation to the mechanism associated with such catalysts using a combination of experimental and theoretical techniques.

2. Experimental

2.1. One-step flame synthesis of CO-PROX catalysts

The Pt–FeO_x–CeO_2 catalysts were synthesized in a two-nozzle FSP setup consisting of two conventional FSP nozzles [42,43]. As shown in Scheme 1, the CeO_2 particles were synthesized in one flame and the Pt–FeO_x particles in the opposing flame. The nozzle separation $|d|$ was varied between small, $|s| = 6.5$ cm (sample Pt–Fe|*s*|Ce), medium, $|m| = 8.4$ cm (sample Pt–Fe|*m*|Ce), and high, $|h| = 12$ cm (sample Pt–Fe|*h*|Ce) distances. The intersection angle of the two nozzles was kept constant at $\alpha = 20°$ to the horizontal. The liquid precursor for the synthesis of CeO_2 (FSP nozzle 1) consisted of 0.22 M cerium(III) 2-ethylhexanoate (49% in 2-ethylhexanoic acid, Strem Chemicals) in xylene (Aldrich), while that for the synthesis of Pt–FeO_x (FSP nozzle 2) consisted of 0.044 M iron(III) 2-ethylhexanoate (52% in mineral spirits, Alfa Aesar) and 0.0107 M platinum(II) acetylacetonate (95%, Aldrich) in xylene. The chosen concentrations resulted in a Ce:Fe ratio of 5:1 and 5 wt.% Pt with respect to the combined oxide weight of CeO_2 and Fe_2O_3. The liquid precursors were delivered at 5 mL min^{-1} to each of the nozzles separately by syringe pumps. At each nozzle, the precursor was atomized by 5 L min^{-1} O_2 (1.5 bar) at the nozzle tip and ignited by a premixed CH_4 (1.5 L min^{-1}) and O_2 (3.2 L min^{-1}) supporting flame to sustain the spray flame. The formed aerosols were collected on a glass fiber filter with the aid of a vacuum pump [36]. In the case of Pt–FeO_x–CeO_2 synthesized in single-nozzle FSP (sample Pt–Fe–Ce), the precursors were combined in a single solution and sprayed in a single flame setting. Similarly, pristine Fe_2O_3 (0.044 M iron(III) 2-ethylhexanoate in xylene), Pt–FeO_x (0.044 M iron(III) 2-ethylhexanoate and 0.0107 M platinum(II) acetylacetonate in xylene), 5%Pt–Fe_2O_3 (0.40 M iron(III) 2-ethylhexanoate and 0.0082 M platinum(II) acetylacetonate in xylene), pristine CeO_2 (0.22 M cerium(III) 2-ethylhexanoate in xylene), and Pt–CeO_2 (0.22 M cerium(III) 2-ethylhexanoate and 0.0107 M platinum(II) acetylacetonate in xylene) were synthesized with the single-nozzle configuration. All FSP-prepared samples were recovered from the glass fiber filters and used as prepared. A physically mixed sample (Pt–Fe|*mix*|Ce) was produced by mechanically mixing Pt–FeO_x powder and CeO_2 in an agate mortar in a Ce:Fe ratio of 5:1.

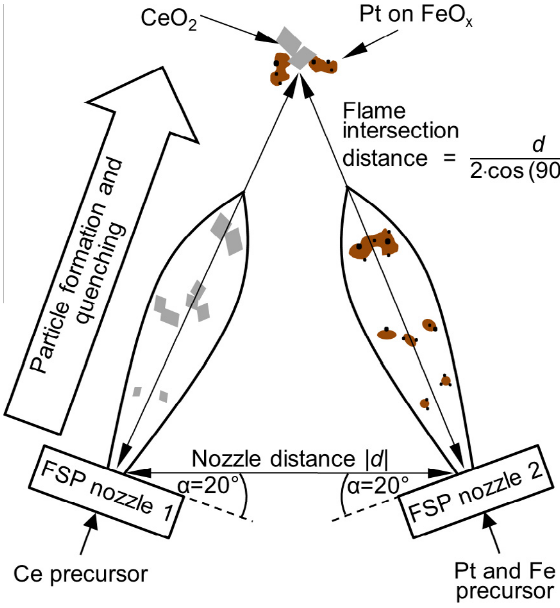

Scheme 1. The two-nozzle flame spray pyrolysis (FSP) reactor utilized for sample synthesis. The Ce precursor solution was introduced into one FSP nozzle while a Pt- and Fe-containing solution was used for the second FSP nozzle. By varying the nozzle distance $|d|$ ($|s| = 6.5$, $|m| = 8.4$, and $|h| = 12$ cm) and thus the flame intersection distance, the formed CeO_2 and Pt–FeO_x nanoparticles mix at different stages of particle formation and at different temperatures.

2.2. Physicochemical characterization of CO-PROX catalysts

X-ray diffraction (XRD) of the as-prepared catalyst powders was performed with a Bruker D8 diffractometer equipped with a secondary monochromator and a Cu K_α ($\lambda = 0.154$ nm) radiation source. An integration step width of $2\theta \sim 0.02°$ was applied at 5 s per step. High-resolution XRD of the Pt–Fe|*h*|Ce sample was performed on a Philips PW1800 diffractometer operating with a monochromated Cu K_α ($\lambda = 0.154$ nm) radiation source and primary and secondary Soller slits and an aperture of 0.1 rad. The step width was 0.04° with a measuring time of 18 s per step.

X-ray photoelectron spectroscopy (XPS) was performed on an ESCALAB 250Xi (Thermo Scientific) equipped with a monochromated Al K_α X-ray source and a pass energy of 20 kV. XPS depth profiles were acquired with 50 kV pass energy while etching with a 3 keV Ar^+ beam (corresponding to a 0.42 nm s^{-1} etching rate, as calibrated with a Ta_2O_5 reference). All binding energies were referenced to the C1*s* line at 285.0 eV.

Scanning transmission electron microscopy (STEM) images of the catalysts were taken with a FEI Titan 80/300 operating at 300 kV and equipped with a high-angle annular dark field (HAADF) detector. Samples were dispersed on carbon-coated copper grids. Selected-area electron diffraction (SAED) patterns were